RSC Advances

PAPER

View Article Online
View Journal | View Issue

Cite this: *RSC Adv.*, 2017, **7**, 55074

Fabrication and evaluation of $Rb_2Co(H_2P_2O_7)_2 \cdot 2H_2O$/waterborne polyurethane nanocomposite coating for corrosion protection aspects

M. A. Deyab, *[a] R. Essehli,[b] B. El Bali[c] and M. Lachkar[c]

Received 11th October 2017
Accepted 27th November 2017

DOI: 10.1039/c7ra11212b

rsc.li/rsc-advances

Here we investigate the influence of new acidic pyrophosphate ($Rb_2Co(H_2P_2O_7)_2 \cdot 2H_2O$) (DP) incorporation in waterborne polyurethane (WBPU) coatings on the corrosion protection efficiency of WBPU coatings for carbon steel in 3.5% NaCl solution. We used potentiodynamic polarization, electrochemical frequency modulation (EFM) and pull-off adhesion and O_2 gas permeability measurements to measure the corrosion protection efficiency of the WBPU coating. The dispersion of the DP nano-particles into the WBPU matrix was characterized *via* TEM observations. We find that the corrosion resistance and mechanical properties of the WBPU coating increase with incorporation of DP nano-particles into the WBPU coating.

1. Introduction

Carbon steel is the most important alloy used in petroleum pipelines. However, its main drawback is corrosion.[1] The integration between cathodic protection and organic coatings can establish long-term protection for petroleum pipelines.[2]

Polyurethane coatings are used in a broad range of construction applications under different conditions, especially on cathodically protected surfaces.[3,4]

Waterborne polyurethane coatings are being progressively used instead of coating with organic solvent to minimize the release of volatile organic solvents.[5] Waterborne polyurethane has been vastly used as an effective coating for protecting metallic surfaces from corrosion.[6]

Polyurethane has hydroscopic susceptibility and lacunar structure which make its coating permeable to aggressive agents.[7] These drawbacks accelerate the corrosion of the metallic substrate over time.[8] In this status, the incorporation of nanoparticles in organic coatings is a favorable approach for enhancing corrosion resistance of polyurethane coatings.[9,10] The improvement of the corrosion resistance and mechanical properties of organic coating using inorganic materials is a promising approach for coating system.[11–13]

Recent works showed that inorganic materials improves the corrosion resistance of organic coatings by enlarging the route of corrosive ions and water in the coating to reach the metal/coating interface and enhance the barrier effects of coating matrix.[14,15]

In our previous works the effects of new inorganic materials on corrosion resistance and mechanical properties of organic coating were studied.[16–20] We proved in these works that the nanoparticles of inorganic materials improve the corrosion resistance and mechanical properties of organic coating. As to continue these investigations, the current work intends to study the effect of the new acidic pyrophosphate $Rb_2Co(H_2P_2O_7)_2 \cdot 2H_2O$ (DP) incorporation in waterborne polyurethane (WBPU) coatings on the corrosion protection efficiency of WBPU coating.

Acidic metal pyrophosphates are characterized by their biological uses. Moreover, they are used as additive in fertilizers, or even in medicine.[21] In acidic pyrophosphates, various oxoanions $(HP_2O_7)^{3-}$, $(H_2P_2O_7)^{2-}$ and $(H_3P_2O_7)^{-}$ are involved in the molecular structure. These oxoanions are interconnected by strong hydrogen bonds, leading to various geometries (*i.e.* chains, ribbons, layers or three-dimensional network).[21]

The practical tests have been conducted on samples of carbon steel immersed in salt solution (3.5% NaCl) and measured by means of electrochemical and mechanical methods.

2. Experimental method

2.1. Materials and chemicals

A carbon steel panel with the following chemical composition: (wt%); 0.06 C; 0.02 Cu; 0.7 Mn; 0.005 P; 0.012 Ni; 0.06 Si; 0.015 Cr; 0.004 Mo; 0.001 S; 0.002 V and Fe (bal.), was used as a metallic substrate. The metallic substrates used in the

[a]Egyptian Petroleum Research Institute (EPRI), P.O. Box 11727, Nasr City, Cairo, Egypt. E-mail: hamadadeiab@yahoo.com

[b]Qatar Environment and Energy Research Institute, Hamad Bin Khalifa University, Qatar Foundation, P.O. Box 5825, Doha, Qatar

[c]Laboratoire d'Ingénierie des Matériaux Organométalliques et Moléculaires «L.I.M.O.M», Faculté des Sciences, Université Sidi Mohamed Ben Abdellah, B. P. 1796 (Atlas), Fès, Morocco

electrochemical experiment were mechanically cut into 3.5 cm × 2.5 cm × 0.3 cm dimensions, then abraded with emery papers up to 1200 grit, and washed with absolute ethanol and acetone.[22] The clean metallic substrates were dried at room temperature and stored in a moisture free desiccator before coating.

Waterborne polyurethane (the solid content is 37 wt%) and isocyanate based hardener were purchased from DOW Chemical Company and Bayer Company, respectively.

The aggressive environment used was 3.5 wt% NaCl solution. All chemicals were of AR grade and the solutions were prepared using deionized water.

2.2. Synthesis of $Rb_2Co(H_2P_2O_7)_2\cdot 2H_2O$

Single crystals of $Rb_2Co(H_2P_2O_7)_2\cdot 2H_2O$ have been prepared in solution dissolving stoechiometrical amounts of Rb_2CO_3 (1 mmol) and $CoCl_2\cdot 6H_2O$ (0.5 mmol) in a solution made of $K_4P_2O_7$ in water (1 mmol). The mixture, to which few drops of concentrated HCl (2 M) were added, has been stirred for 4 h, and the resulting solution was stored at room temperature. After one week, well shaped pink crystals deposited, which have been filtered off and washed with a mixture ethanol–water (80 : 20).

2.3. Preparation of WBPU/DP nano-particles coating

Crystals of the DP were thoroughly grounded and sieved as to get nanoparticles, these were added into the waterborne polyurethane in different concentrations to obtain 0.2%, 0.5% and 1.0% by weight in the final coating formula. DP nano-particles were completely dispersed in WBPU coatings by mechanical stirring at 1500 rpm for 40 min, followed by ultrasonication process for about 15 min. Isocyanate based hardener was added to the coating formula at 1 : 3 ratio to prepare a homogeneous and stable coating formula.

There are limitations of adding nano-particles above 1.0%, because of homogeneity and to slow down nano-particles re-aggregation after mechanical stirring removal.

2.4. Characterization

A single crystal was selected and X-ray diffraction (XRD) data were collected on an Oxford Diffraction XCALIBUR four-circles X-ray diffractometer using graphite monochromatized MoKα radiation ($\lambda = 0.7173$ Å) equipped with a SAPPHIR CCD two-dimensional detector.

A transmission electron microscope (Model: Jeol-Jem 1200EX II equipped with TEM) was used to determine the size of DP nano-particles and to evaluate the dispersion and distribution of DP nano-particles in WBPU.

2.5. Preparation of the coated substrates

The prepared coatings were applied on clean carbon steel panels by conventional spraying process. The thickness of dry coating film (measured by hand held micrometer, B.C. Ames Co.) was in the range of 65 ± 10 μm. The coated substrates were stored in a moisture free desiccator before testing.

2.6. Electrochemical experiments

The Corrosion resistance property of coatings was conducted using potentiodynamic polarization and EFM measurements.

The electrochemical set-up composed of three electrodes layout in a glass cell, with a Pt counter electrode and a saturated calomel reference electrode (SCE). The experiments were conducted in a 100 ml volume cell at 298 K using a temperature control water bath.

All electrochemical measurements were carried out with ACM instruments Potentiostat/Galvanostat (Gill AC Serial no. 947).

For potentiodynamic polarization experiments, open circuit potential (OCP) of system after immersion for 2 h and 7 days in corrosive solution was recorded. Then, the Tafel plot was plotted by sweeping the applied potential from −0.25 to +0.25 V with respect to OCP with a constant sweep rate of 1.0 mV s^{-1}. EFM measurements were implemented by applying potential perturbation signal with amplitude of 10 mV with two sine waves of 2 and 5 Hz.

All electrochemical experiments were performed in triplicate to guarantee reproducibility of the results and the mean values were recorded.

2.7. Pull-off adhesion experiments

Pull-off adhesion testers (PAT model GM01/6.3 kN) was used to determine the adhesion strength of WBPU coatings coatings after 10 days of immersion in 3.5 wt% NaCl solution. All the experiments were repeated three times, and good reproducibility of the results was observed.

2.8. O_2 gas barrier property experiments

O_2 gas barrier property of prepared coating was determined at 298 K using Oxygen Permeation Analyzers (model 8501, Illinois Instruments, Inc.). The measurements were occurred according ASTM D3985 standard test methods.

3. Results and discussion

3.1. Crystal structure

$Rb_2Co(H_2P_2O_7)_2\cdot 2H_2O$ is isostructural to $Rb_2M(H_2P_2O_7)_2\cdot 2H_2O$ (M = Mg, Zn).[21] It crystallizes in the triclinic system ($P\bar{1}$). Its crystal structure might be desribed as a 3D framework made of corners and/or edges sharing $[RbO_7]$, $[CoO_4(H_2O)_2]$ and $[H_2P_2O_7]$ polyedra, Fig. 1 depicts a projection of the crystal structure onto (010). In another view, $[CoO_4(H_2O)_2]$ is coordinated by two bidentate $[H_2P_2O_7]$ pyrophosphate groups to form the phosphocobaltate $[Co(H_2P_2O_7)_2\cdot 2H_2O]$ entity. These entities are linked through Rb–O interactions, and intricate H-bonds from the hydroxyl groups, to extend tridimentionally. Fig. 2 shows the coordination scheme around the metals in the framework of the title compound.

$Rb_2Co(H_2P_2O_7)_2\cdot 2H_2O$ crystallizes in the triclinic system ($P\bar{1}$) with the cell parameters (Å, °): 6.980(1), 7.370(1), 7.816(1), 81.74(1), 70.35(1), 86.34(1); $V = 374.68(9)$ Å^3, $Z = 2$.

Further details on the crystal structure investigations of the title compound might be obtained from the Inorganic Crystal

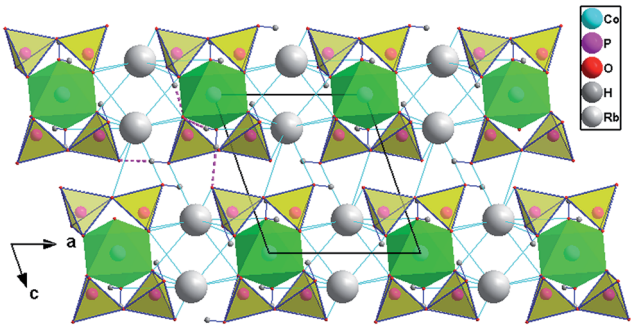

Fig. 1 $Rb_2Co(H_2P_2O_7)_2\cdot 2H_2O$, a projection of the framework onto crystallographic plane (010), H-bonds as dashed lines.

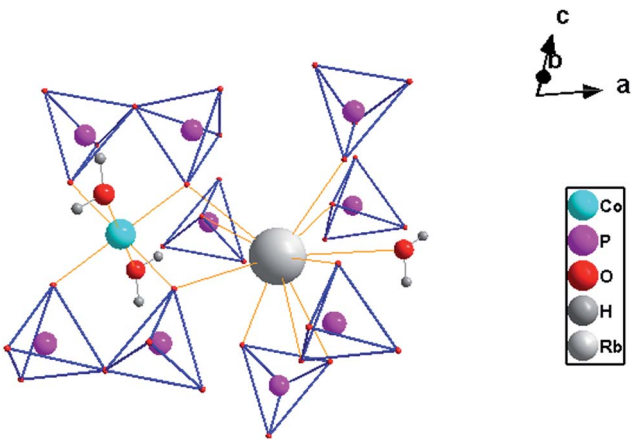

Fig. 2 Metal coordination in $Rb_2Co(H_2P_2O_7)_2\cdot 2H_2O$, for clarity only one tetrahedron from $[H_2P_2O_7]$ is presented around Rb.

Structure Database, FIZ, Hermann von Helmholtz Platz 1, 76344 Eggenstein-Leopoldshafen, Germany; fax: (+49) 7247 808 132; http://www2.fiz-karlsruhe.de/icsd_home.html, on quoting the depository number CSD 421807.

3.2. TEM observation

The TEM image of DP nano-particles is shown in Fig. 3. The TEM analysis demonstrates that the particle size of DP nano-particles was found to be around 70 nm.

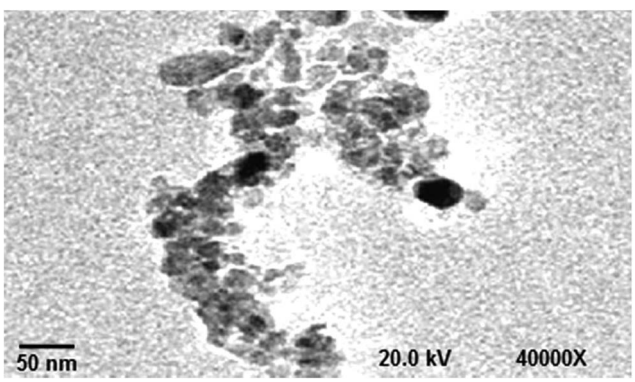

Fig. 3 TEM image of DP nano-particles.

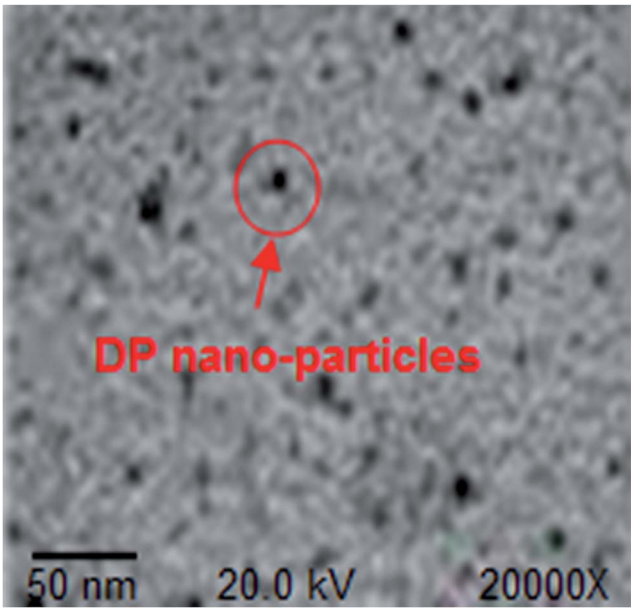

Fig. 4 TEM image of WBPU/DP nano-particles nanocomposite.

The TEM image of WBPU/DP nano-particles nanocomposite (see Fig. 4) confirms that the DP nano-particles were uniformly dispersed in the WBPU matrix.

3.3. Corrosion resistance property of WBPU coating in the presence of $Rb_2Co(H_2P_2O_7)_2\cdot 2H_2O$

3.3.1 Polarization measurements. Potentiodynamic polarization test (Tafel plot) was employed to study the effect of the incorporation of $Rb_2Co(H_2P_2O_7)_2\cdot 2H_2O$ nanoparticles with the coating on the corrosion resistance property of WBPU coatings after exposure to the saline solution (3.5% NaCl) (Fig. 5). The polarization curves were obtained after stabilization for 2 h and

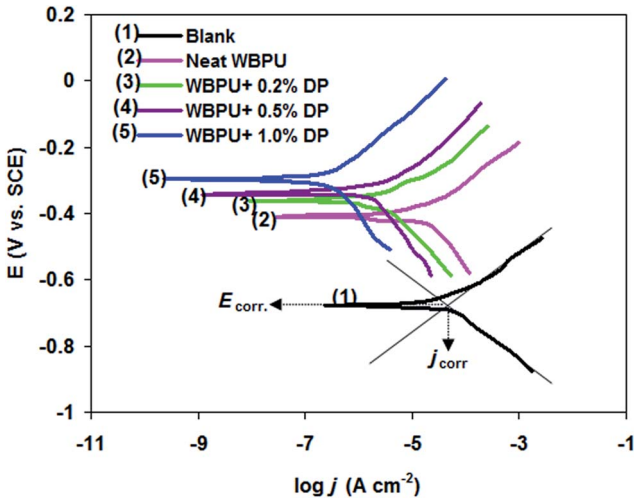

Fig. 5 Tafel plots for carbon steel coated by waterborne polyurethane (WBPU) coating containing pyrophosphate (DP) after 2 h of immersion in 3.5% NaCl solution at 298 K.

the electrochemical parameters (corrosion potential E_{corr} and corrosion current density j_{corr}) obtained from polarization curves are presented in Table 1.

The E_{corr} of bare carbon steel is about −0.676 with j_{corr} of about 63.09 μA cm^{-2}. In the case of neat WBPU coating, E_{corr} shifts to more positive potentials (−0.411 V) and j_{corr} decreases to 13.08 μA cm^{-2}, confirming that the coated carbon steel substrate by neat WBPU coating is still susceptible to corrosion to some extent. On the other hand, WBPU + DP coated substrate exhibits more positive E_{corr} with a remarkable decrease of j_{corr} (Table 1). The noble shift of E_{corr} accompanying with decrease of j_{corr}, suggest that the incorporation of different concentrations of DP nano-particles into WBPU coating improves the corrosion resistance of the mild carbon steel substrate remarkably.[23]

The protection efficiency (η_j%) of the coatings was defined as:[24,25]

$$\eta_j\% = \frac{j^{o}_{corr} - j^{c}_{corr}}{j^{o}_{corr}} \times 100 \quad (1)$$

where j^{o}_{corr} and j^{c}_{corr} are the corrosion current densities in the absence and presence of coatings, respectively.

The calculated η_j% values obtained from polarization measurements are listed in Table 1. The protection efficiency η_j% of the WBPU + DP coatings was found to be significantly increased as compared to neat WBPU (Table 1). The η_j% of the WBPU + DP coatings was increased as the percentage of DP nano-particles increased. Coated carbon steel sample with WBPU + 1.0% DP, showed the highest the corrosion resistance (η_j% = 99.60).

In addition, coatings have been modified with nano-particles to achieve desirable properties such as increased adhesion and cohesion.[26] Here, cohesion reflects the strength and fracture resistance of the coating material, while adhesion indicates the interfacial bond strength of coatings or adhesives.[27] This improvement in the corrosion resistance of WBPU coating in the presence of DP nano-particles is attributed to; DP nano-particles are well dispersed in WBPU coating, which restrict the diffusion of the corrosive ions and water through the WBPU coating film.[28,29] Moreover, the large surface area and the small size of DP nano-particles, absorb more WBPU coating on its surface which reinforces the density of the WBPU coating films, that way the transport paths for the corrosive ions and water to pass through the WBPU coating become longer and consequently inhibiting the corrosion process.[30]

Table 1 Electrochemical parameters and the corresponding protection efficiency for carbon steel coated by waterborne polyurethane (WBPU) coating containing pyrophosphate (DP) immersed in 3.5% NaCl solution at 298 K

Samples	E_{corr} V (*vs.* SCE)	j_{corr} μA cm^{-2}	η_j%
Bare carbon steel	−0.676	63.09	—
Neat WBPU	−0.411	13.08	79.26
WBPU + 0.2% DP	−0.363	4.43	92.97
WBPU + 0.5% DP	−0.342	2.28	96.38
WBPU + 1.0% DP	−0.292	0.25	99.60

The effect of long time immersion of WBPU + 1.0% DP coating was shown in Fig. 6. It is observed that after immersion of the coated carbon steel by WBPU + 1.0% DP, there is a slightly increase in the magnitude of the corrosion current (from 0.25 μA cm^{-2} to 2.9 μA cm^{-2}) with increasing the immersion time from 2 h to 7 days. This is referring to the high corrosion resistance nature of the WBPU + 1.0% DP coating.

3.3.2 Electrochemical frequency modulation. Electrochemical Frequency Modulation (EFM) is a powerful non-destructive method for measuring the corrosion rate of coating system. The EFM technique was used for monitoring of the corrosion rate of various types of corroding systems within reasonable time without prior knowledge of Tafel parameters by applying a small polarizing signal.

The EFM intermodulation spectra of uncoated and coated carbon steel by WBPU coating containing DP nano-particles immersed in 3.5% NaCl solution at 298 K are shown in Fig. 7. The parameters obtained from EFM spectra ($j_{corr(EFM)}$ and the causality factors CF2, CF3) are listed in Table 2.

It seems that the values of the causality factors CF2, CF3 for uncoated and coated carbon steel substrates are around the theoretical values (2 and 3), signifying the accuracy of the obtained results.[31]

According to Table 2, all coated carbon steel show higher $j_{corr(EFM)}$ than uncoated substrates; meanwhile, WBPU coatings containing DP nano-particles show significantly greater $j_{corr(EFM)}$ values. From EFM data, the protection efficiency (η_{EFM}%) of the coatings can be calculated using eqn (2):[32]

$$\eta_{EFM}\% = \frac{j^{o}_{corr(EFM)} - j^{c}_{corr(EFM)}}{j^{o}_{corr(EFM)}} \times 100 \quad (2)$$

where $j^{o}_{corr(EFM)}$ and $j^{c}_{corr(EFM)}$ are the corrosion current densities obtained by EFM data in the absence and presence of coatings respectively.

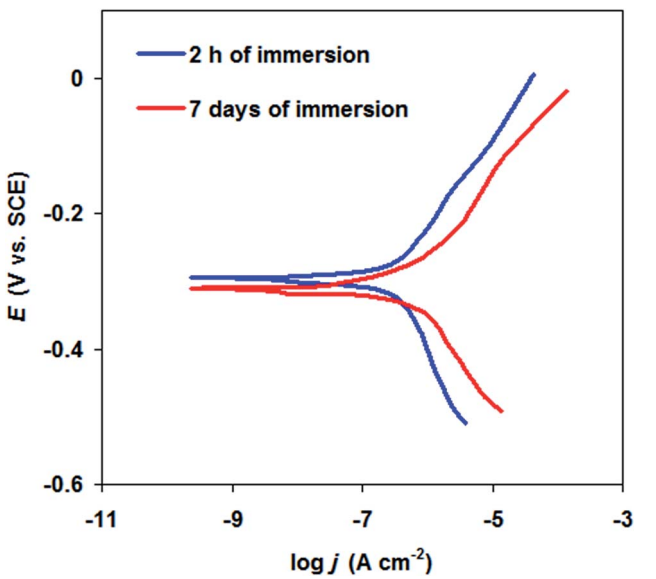

Fig. 6 Tafel plots for carbon steel coated by WBPU + 1.0% DP after 2 h and 7 days of immersion in 3.5% NaCl solution at 298 K.

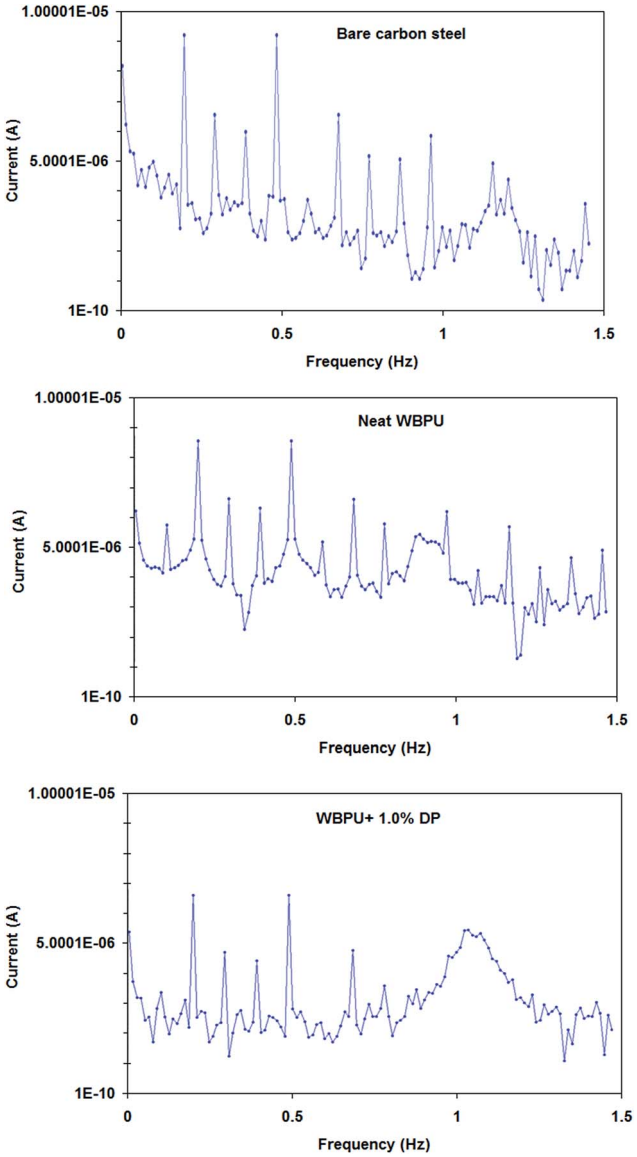

Fig. 7 EFM intermodulation spectra of uncoated and coated carbon steel by WBPU coating containing DP nano-particles immersed in 3.5% NaCl solution at 298 K.

Table 2 Electrochemical kinetic parameters obtained by EFM technique, and the corresponding protection efficiency for carbon steel coated by waterborne polyurethane (WBPU) coating containing pyrophosphate (DP) immersed in 3.5% NaCl solution at 298 K

Samples	CF2	CF3	$j_{corr(EFM)}$ μA cm^{-2}	η_{EFM}%
Bare carbon steel	1.77	2.44	69.32	—
Neat WBPU	1.84	2.67	19.38	72.04
WBPU + 0.2% DP	1.89	2.84	7.94	88.54
WBPU + 0.5% DP	1.91	2.75	4.85	93.00
WBPU + 1.0% DP	1.93	2.82	1.99	97.12

The calculated η_{EFM}% values are listed in Table 2. According to these results, DP nano-particles tend to agglomerate in WBPU matrix by increasing DP wt%. The WBPU coating with 0.1 wt% DP nano-particles shows the best corrosion protection performance (97.12%). This is consistent with the finding that obtained from polarization measurements.

3.4. Mechanical property of WBPU coating in the presence of $Rb_2Co(H_2P_2O_7)_2 \cdot 2H_2O$

The mechanical property of WBPU coating in the absence and presence of DP nano-particles is conducted using pull-off adhesion measurements and the results are presented in Fig. 8. The average pull-off adhesion strength of WBPU coatings enhances by incorporation of different amount of DP nano-particles. The average adhesion strength of the WBPU coating without DP nano-particles was 3.2 MPa, while average adhesion strengths of 6.6 MPa, 8.8 and 10.5 MPa were obtained at 0.2 wt%, 0.5% wt% and 1.0 wt% of DP nano-particles, respectively.

The adhesion strength of WBPU highly depends on the chain extenders and their content.[33] Neat WBPU coating adheres to carbon steel surface *via* chemical adhesion supported by mechanical interlocking adhesion. The reactive functional groups of WBPU coating such as NH and CO groups tend to adhere to carbon steel surface *via* formation of chemically bond.[34] In these applications the formation of covalent chemical bonds occurs across the interface. Coating systems containing reactive functional groups tend to adhere more strongly to metal surface containing similar reactive functional groups.[23]

The incorporation of DP nano-particles is also believed to diminish the porosity of the WBPU coating.[35,36] Moreover, the DP nano-particles can suppresses the coating cracking when the WBPU coating is exposed to an external stress and it will result in the improvement of the coating flexibility. This causes better adhesion of WBPU coatings containing DP nano-particles than neat WBPU.

3.5. O_2 gas barrier property of WBPU coating in the presence of $Rb_2Co(H_2P_2O_7)_2 \cdot 2H_2O$

O_2 gas permeability of WBPU coating in the absence and presence of DP nano-particles at 298 K was presented in Table 3. The

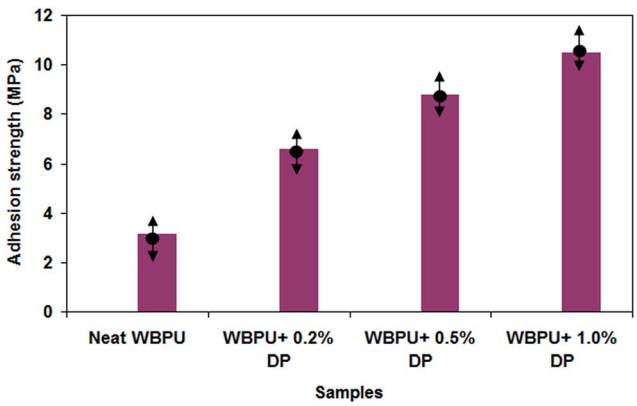

Fig. 8 Pull-off adhesion of the coatings of WBPU-coated carbon steel in the absence and presence of different concentrations of DP nano-particles.

Table 3 O_2 gas permeability of WBPU coating in the absence and presence of $Rb_2Co(H_2P_2O_7)_2 \cdot 2H_2O$ at 298 K

Coating type	O_2 permeability (cc m^{-2} day)
Neat WBPU	48.3
WBPU + 0.2% DP	13.4
WBPU + 0.5% DP	5.5
WBPU + 1.0% DP	4.0

incorporation of DP nano-particles into WBPU coating causes a significant decrease in the permeation of oxygen across the coating thickness. The best barrier performance was recorded for the coating with the highest concentration of $Rb_2Co(H_2P_2O_7)_2 \cdot 2H_2O$ (*i.e.* WBPU + 1.0% DP). It has been explained on the basis that the incorporation of DP nano-particles into WBPU coating can create a tortuous path for O_2 gas molecules. This causes an increase of the total path of the gas.[37] This results support the corrosion protection data.

4. Conclusions

The effect of nano-particles of new acidic pyrophosphates ($Rb_2Co(H_2P_2O_7)_2 \cdot 2H_2O$) on the corrosion protection efficiency of WBPU coatings for carbon steel in saline solution (3.5% NaCl) was assessed by electrochemical and mechanical methods. Potentiodynamic polarization and EFM curves proved that the addition of DP nano-particles had improved the corrosion protection performance of WBPU coating. Increment of the DP nano-particles concentration exhibited a significant effect on the coating performance. The superior the corrosion protection efficiency of the WBPU coating was achieved by the addition of 1.0 wt% of DP nano-particles. Further, WBPU coating containing DP nano-particles showed the highest pull-off adhesion strength, demonstrating the enhanced mechanical performance of WBPU coating with the addition of DP nano-particles.

Conflicts of interest

There are no conflicts to declare.

References

1 M. A. Deyab, The influence of different variables on the electrochemical behavior of mild steel in circulating cooling water containing aggressive anionic species, *J. Solid State Electrochem.*, 2009, **13**, 1737–1742.
2 A. S. Ismail, Nano-sized aluminum coatings from aryl-substituted imidazolium cation based ionic liquid, *Egypt. J. Pet.*, 2016, **25**, 525–530.
3 S. Huang, J. Xiao, Y. Zhu and J. Qu, Synthesis and properties of spray-applied high solid content two component polyurethane coatings based on polycaprolactone polyols, *Prog. Org. Coat.*, 2017, **106**, 60–68.
4 J. V. Nardeli, D. V. Snihirova, C. S. Fugivara, M. F. Montemor, E. R. P. Pinto, Y. Messaddecq and A. V. Benedetti, Localised corrosion assessement of crambe-oil-based polyurethane coatings applied on the ASTM 1200 aluminum alloy, *Corros. Sci.*, 2016, **82**, 422–435.
5 J. Li, J. Cui, J. Yang, Y. Li, H. Qiu and J. Yang, Reinforcement of graphene and its derivatives on the anticorrosive properties of waterborne polyurethane coatings, *Compos. Sci. Technol.*, 2016, **129**, 30–37.
6 J. Y. Kwon and H. D. Kim, Preparation and properties of acid-treated multiwalled carbon nanotube/waterborne polyurethane nanocomposites, *J. Appl. Polym. Sci.*, 2005, **96**, 595–604.
7 Y. Li, Z. Yang, H. Qiu, Y. Dai, Q. Zheng, J. Li and J. Yang, Self-aligned graphene as anticorrosive barrier in waterborne polyurethane composite coatings, *J. Mater. Chem. A*, 2014, **2**, 14139–14145.
8 O. C. Compton, S. Kim, C. Pierre, J. M. Torkelson and S. T. Nguyen, Crumpled grapheme nanosheets as highly effective barrier property enhancers, *Adv. Mater.*, 2010, **22**, 4759–4763.
9 G. Christopher, M. A. Kulandainathan and G. Harichandran, Biopolymers nanocomposite for material protection: Enhancement of corrosion protection using waterborne polyurethane nanocomposite coatings, *Prog. Org. Coat.*, 2016, **99**, 91–102.
10 M. A. Deyab, Effect of carbon nano-tubes on the corrosion resistance of alkyd coating immersed in sodium chloride solution, *Prog. Org. Coat.*, 2015, **85**, 146–150.
11 P. Li, X. He, T.-C. Huang, K. L. White, X. Zhang, H. Liang, R. Nishimura and H.-J. Sue, Highly effective anti-corrosion epoxy spray coatings containing self-assembled clay in smectic order, *J. Mater. Chem. A*, 2015, **3**, 2669–2676.
12 P. Sambyal, G. Ruhi, R. Dhawan and S. K. Dhawan, Designing of smart coatings of conducting polymer poly(aniline-co-phenetidine)/SiO_2 composites for corrosion protection in marine environment, *Surf. Coat. Technol.*, 2016, **303**, 362–371.
13 J.-M. Yeh, S.-J. Liou, C.-Y. Lai, P.-C. Wu and T.-Y. Tsai, Enhancement of Corrosion Protection Effect in Polyaniline via the Formation of Polyaniline–Clay Nanocomposite Materials, *Chem. Mater.*, 2001, **13**, 1131–1136.
14 K. Qi, Y. Sun, H. Duan and X. Guo, A corrosion-protective coating based on a solution-processable polymer-grafted graphene oxide nanocomposite, *Corros. Sci.*, 2015, **98**, 500–506.
15 A. Yabuki and M. Sakai, Self-healing coatings of inorganic particles using a pH-sensitive organic agent, *Corros. Sci.*, 2011, **53**, 829–833.
16 M. A. Deyab, R. Ouarsal, A. M. Al-Sabagh, M. Lachkar and B. El Bali, Enhancement of corrosion protection performance of epoxy coating by introducing new hydrogenphosphate compound, *Prog. Org. Coat.*, 2017, **107**, 37–42.
17 M. A. Deyab, G. Mele, A. M. Al-Sabagh, E. Bloise, D. Lomonaco, S. E. Mazzetto and C. D. S. Clemente, Synthesis and characteristics of alkyd resin/M-Porphyrins nanocomposite for corrosion protection application, *Prog. Org. Coat.*, 2017, **105**, 286–290.

18 M. A. Deyab, K. Eddahaoui, R. Essehli, S. Benmokhtar, T. Rhadfi, A. De Riccardis and G. Mele, Influence of newly synthesized titanium phosphates on the corrosion protection properties of alkyd coating, *J. Mol. Liq.*, 2016, **216**, 699–703.

19 M. A. Deyab, A. De Riccardis and G. Mele, Novel epoxy/metal phthalocyanines nanocomposite coatings for corrosion protection of carbon steel, *J. Mol. Liq.*, 2016, **220**, 513–517.

20 M. A. Deyab, A. A. Nada and A. Hamdy, Comparative study on the corrosion and mechanical properties of nano-composite coatings incorporated with TiO_2 nano-particles, TiO_2 nano-tubes and ZnO nano-flowers, *Prog. Org. Coat.*, 2017, **105**, 245–251.

21 R. Essehli, B. El Bali, M. Lachkar and G. Cruciani, Two new acidic diphosphates $Rb_2M(H_2P_2O_7)_2 \cdot 2H_2O$ (M= Zn and Mg): Crystal structures and vibrational study, *J. Alloys Compd.*, 2010, **492**, 358–362.

22 M. A. Deyab and S. T. Keera, Cyclic voltammetric studies of carbon steel corrosion in chloride-formation water solution and effect of some inorganic salts, *Egypt. J. Pet.*, 2012, **21**, 31–36.

23 S. Pourhashem, M. R. Vaezi, A. Rashidi and M. R. Bagherzadeh, Exploring corrosion protection properties of solvent basedepoxy-graphene oxide nanocomposite coatings on mild steel, *Corros. Sci.*, 2017, **115**, 78–92.

24 C. Xing, Z. Zhang, L. Yu, L. Zhangb and G. A. Bowmaker, Electrochemical corrosion behavior of carbon steel coated by polyaniline copolymers micro/nanostructures, *RSC Adv.*, 2014, **4**, 32718–32725.

25 K.-C. Chang, S.-T. Chen, H.-F. Lin, C.-Y. Lin, H.-H. Huang, J.-M. Yeh and Y.-H. Yu, Effect of clay on the corrosion protection efficiency of PMMA/Na+-MMT clay nanocomposite coatings evaluated by electrochemical measurements, *Eur. Polym. J.*, 2008, **44**, 13–23.

26 M. K. Madhup, N. K. Shah and N. R. Parekh, The Effect of Zinc Oxide Nanoparticles on Cohesive and Adhesive Bond of Epoxy/Amine Coating on Carbon Steel Substrate, *J. Appl. Chem.*, 2017, **10**, 47–58.

27 R. Lacombe, *Adhesion measurement methods: theory and practice*, CRC Press, Boca Raton, 2006.

28 B. A. Bhanvase and S. H. Sonawane, New approach for simultaneous enhancement of anticorrosive and mechanical properties of coatings: Application of water repellent nano $CaCO_3$–PANI emulsion nanocomposite in alkyd resin, *Chem. Eng. J.*, 2010, **156**, 177–183.

29 L. Ejenstam, M. Tuominen, J. Haapanen, J. M. Mäkelä, J. Pan, A. Swerin and P. M. Claesson, *Appl. Surf. Sci.*, 2015, **357**, 2333–2342.

30 L. H. Yang, F. C. Liu and E. H. Han, Effects of P/B on the properties of anticorrosive coatings with different particle size, *Prog. Org. Coat.*, 2005, **53**, 91–99.

31 E. B. Ituen, A. O. James and O. Akaranta, Fluvoxamine-based corrosion inhibitors for J55 steel in aggressive oil and gas well treatment fluids, *Egypt. J. Pet.*, 2017, **26**, 745–756.

32 M. A. Amin, M. A. Ahmed, H. A. Arida, T. Arslan, M. Saracoglu and F. Kandemirli, Monitoring corrosion and corrosion control of iron in HCl by non-ionic surfactants of the TRITON-X series – Part II. Temperature effect, activation energies and thermodynamics of adsorption, *Corros. Sci.*, 2011, **53**, 540–548.

33 S. Mohammadi, F. A. Taromi, H. Shariatpanahi, J. Neshati and M. Hemmati, Electrochemical and anticorrosion behavior of functionalized graphitenanoplatelets epoxy coating, *J. Ind. Eng. Chem.*, 2014, **20**, 4124–4139.

34 M. M. Rahman, M. H. Zahir and H. D. Kim, Synthesis and Properties of Waterborne Polyurethane (WBPU)/Modified Lignin Amine (MLA) Adhesive: A Promising Adhesive Material, *Polymers*, 2016, **8**, 318–329.

35 P. A. Sørensen, S. Kiil, K. Dam-Johansen and C. E. Weinell, Anticorrosive coatings: a review, *J. Coat. Technol. Res.*, 2009, **6**, 135–176.

36 Y. Hao, F. Liu, H. Shi, E. Han and Z. Wang, The influence of ultra-fine glass fibers on the mechanical and anticorrosion properties of epoxy coatings, *Prog. Org. Coat.*, 2011, **71**, 188–197.

37 M. Oner, A. A. Çol, C. Pochat-Bohatierb and M. Bechelany, Effect of incorporation of boron nitride nanoparticles on the oxygen barrier and thermal properties of poly(3-hydroxybutyrate-cohydroxyvalerate), *RSC Adv.*, 2016, **6**, 90973–90981.